PONTIFICIA UNIVERSIDAD CATOLICA DE CHILE
SCHOOL OF ENGINEERING

DISCRETE-TIME NOISE FILTERING FOR PULSE-PROCESSING IN PARTICLE PHYSICS EXPERIMENTS

DIEGO ÁVILA GÁRATE

Thesis submitted to the Office of Research and Graduate Studies
in partial fulfillment of the requirements for the degree of
Master of Science in Engineering

Advisor: ÁNGEL ABUSLEME HOFFMAN

Santiago de Chile, April 2014

PONTIFICIA UNIVERSIDAD CATOLICA DE CHILE
SCHOOL OF ENGINEERING

DISCRETE-TIME NOISE FILTERING FOR PULSE-PROCESSING IN PARTICLE PHYSICS EXPERIMENTS

DIEGO ÁVILA GÁRATE

Members of the Committee:
ÁNGEL ABUSLEME HOFFMAN
MARCELO GUARINI HERMANN
PROFESOR INVITADO
REPRESENTANTE DE POSTGRADO

Thesis submitted to the Office of Research and Graduate Studies
in partial fulfillment of the requirements for the degree of
Master of Science in Engineering

Santiago de Chile, April 2014

Giggity giggity ...

GLEN QUAGMIRE

ACKNOWLEDGEMENTS

ESCRIBIR AGRADECIMIENTOS

TABLE OF CONTENTS

ACKNOWLEDGEMENTS iv

TABLE OF CONTENTS v

LIST OF FIGURES vii

LIST OF TABLES viii

ABSTRACT ix

RESUMEN x

1. INTRODUCTION 1
   1.1 Particle physics experiments 1
   1.2 Electronics for particle physics experiments 1
   1.3 Noise minimization in circuits for particle physics instrumentation 1
   1.4 Thesis content 2

2. PROBLEM DEFINITION 3
   2.1 The International Linear Collider 3
   2.2 The Bean 3
   2.3 Noise analysis in discrete-time filters 3
   2.4 Arbitrary weighting function synthesis 3

3. NOISE ANALYSIS IN PULSE-PROCESSING DISCRETE-TIME FILTERS . 4
   3.1 Introduction 4
   3.2 Discrete-Time Analysis 5
   3.3 Example 10
   3.4 ENC Minimization 14
   3.5 Conclusion 18

4. A SC FILTER FOR ARBITRARY WEIGHTING FUNCTION SYNTHESIS . 20

4.1 Introduction 20
4.1.1 Filter Specifications 20
4.2 System-Level Design 20
4.3 Circuit Design 20
4.3.1 Operational Transconductance Amplifier 20
4.3.2 Capacitor Array 20
4.3.3 Rail-to-Rail buffer 20
4.3.4 Bias networks 20

5. RESULTS 21
5.1 Filter simulation results 21
5.1.1 OTA simulations results 21
5.1.2 Rail-to-rail buffer simulations results 21
5.1.3 Arbitrary weighting function synthesis 21
5.2 The Bean V2 Prototype 21
5.2.1 Floorplan 21

6. CONCLUSION 22
6.1 Summary 22
6.2 Future work 22

A. The Bean V2 pinout 28

References 24

APPENDIX 27

A. The Bean V2 pinout 28

LIST OF FIGURES

3.1 Model for noise analysis in a typical front-end circuit. 6

3.2 Noise contribution of the pulses generated within P_i and measured at an arbitrary sample k (i.e., $t = kT_s$), using an arbitrary filtered noise core function $\hat{y}(t)$. The independent contribution of each pulse is pointed out with black dots. 8

3.3 Evolution of the total integrated noise at the filter input, where the noise of each sample was split according to (3.10). 10

3.4 $\sigma^2(t)$ for thermal, shot and flicker noise with normalized time t/τ and an arbitrary amplitude. 10

3.5 Front-end circuit used for noise analysis. 11

3.6 $\hat{\sigma}^2_{\text{th}}(N)$ and $N\frac{\overline{v_n^2}}{2\hat{\tau}}\frac{C_{tot}^2}{C_F^2}$ as a function of $\hat{\tau}$, using $\overline{v_n^2} = 1$, $C_{tot}^2/C_F^2 = 1$ and $N = 20$. 13

3.7 Minimum ENC^2 as a function of $\hat{\tau}$ for a fixed N. 17

3.8 Optimum WF for different values of $\hat{\tau}$ for $N = 20$. 17

3.9 Optimum ENC^2 as a function of N for $\hat{\tau} = 0.03\,\mu$s. 18

LIST OF TABLES

ABSTRACT

ESCRIBIR ABSTRACT

Keywords: KEYWORDS

RESUMEN

ESCRIBIR RESUMEN

Palabras Claves: PALABRAS CLAVE

1. INTRODUCTION

1.1 Particle physics experiments

Particle physics, also called High Energy Physics, is the branch of physics that studies the fundamental constituents of matter and radiation, and their mutual interactions. It aims to answer some of the profound questions of physics, with benefits spanning everything from advancing humankind's understanding of the universe, to applications in other fields of science as well as daily life (Tuttle, 2013).

The main tools used by experimental particle physicists are particle accelerators, devices that uses electromagnetic fields to accelerate charged particles to relativistic speeds and to contain them in well-defined beams (Livingston & Blewett, 1962). This beams of are used to generate particle collisions, which can be of a single beam against a stationary target or two beams directed against each other, that's why in the context of particle physics particle accelerators are best known as colliders.

Explicar por que es necesario crear colisionadores mas grandes y sofisticados.

1.2 Electronics for particle physics experiments

Explicar lo que es un detector de partículas y hablar de el front-end de un detector,

1.3 Noise minimization in circuits for particle physics instrumentation

Explicar que el ruido limita la resolución de un detector, explicar de las bases del análisis de ruido, explicar los avances, x ejemplo las nuevas técnicas para minimizar el ruido del amplificador de carga, explicar los nuevos usos y la introducción de filtros discretos.

1.4 Thesis content

Chapter 2 starts with an introduction to the project that prompt the work of this thesis, the design and implementation of a second iteration of The Bean, an instrumentation ASIC which forms part of the proposal for a new particle accelerator, The International Linear Collider (ILC). Its followed by an overview of the motivations that lead to the development of a new mathematical framework for noise analysis in discrete-time filters, alongside with the presentation of the requeriments for a filter intended to take full advantage of this framework. Chapter 3 presents the complete formulation of this noise analysis, including examples and applications for optimal filter computation. In Chapter 4 , the design and implementation of a filter for arbitrary weighting function synthesis are presented, including a detailed description of the

Chapter 6 summarizes the conclusions

in the discrete-time domain.

intended to be used in the next

the design and implementation of an instrumentation ASIC

to

Main work of this thesis

Chapter 2 includes an overview of the detector system in which

2. PROBLEM DEFINITION

2.1 The International Linear Collider

2.2 The Bean

2.3 Noise analysis in discrete-time filters

2.4 Arbitrary weighting function synthesis

3. NOISE ANALYSIS IN PULSE-PROCESSING DISCRETE-TIME FILTERS

3.1 Introduction

In particle physics experiments, where the results from the collisions are inferred from the measurement of electric charge in various sets of detectors (Gatti & Manfredi, 1986; Radeka, 1988), noise sets a fundamental limit for the charge measurement resolution (Geronimo, O'Connor, Radeka, & Yu, 2001). In such experiments, the typical detector front-end circuit comprises a charge-sensitive amplifier (CSA) and a filter, often referred to as pulse shaper. The former is used to convert the input charge signal, coming from the detector electrodes, into a voltage signal, and is responsible for most of the noise present in the readout circuit signal path (De Geronimo & O'Connor, 2005; Geronimo et al., 2001). The filter is used to convert the voltage signal at the CSA output into a shaped voltage pulse, in order to maximize the signal-to-noise ratio (SNR) at the measurement time.

Different noise analysis methods have been proposed to guide a proper filter design. The outcome of these methods is the equivalent noise charge (ENC), a measure of the front-end noise defined as the charge required at the detector input to produce an output SNR of 1. A time-domain analysis based on the weighting function (WF) concept (Goulding, 1972; Radeka, 1988) has long been the preferred analysis, since it allows to find the optimum filter for a wide range of detector configurations (Gatti, Geraci, & Ripamonti, 1996; Geraci & Gatti, 1995; Pullia, 1997; Pullia & Gatti, 2002; Radeka, 1968).

Traditionally, the filter synthesis has been performed using continuous-time networks. However, since producing arbitrary WFs by means of continuous-time analog circuitry is often impossible (Gatti et al., 1996), this approach does not always allow to synthesize optimum filters. A different approach based on discrete-time filters, implemented by means of digital signal processor (DSP) units (Geraci, Zambusi, & Ripamonti, 1996;

Jordanov, 2003; Sampietro, Bertuccio, Geraci, & Fazzi, 1995) or switched capacitor networks (Abusleme, Dragone, Haller, & Wooley, 2012; Fiorini & Buttler, 2002; Porro, Hermann, & Hornel, 2007), allows to synthesize WFs with virtually any shape, producing near-optimum filters. Moreover, this promising approach takes advantage of the aggressive technology scaling and the new techniques of the VLSI industry, allowing to implement fast, reliable and flexible filters.

In this work, a mathematical framework for a design-oriented analysis of discrete-time filters in the discrete-time domain is presented. Although discrete-time filters can be analyzed using a continuous-time method, it is not insightful and the resulting expressions are complex and difficult to use for design purposes. Furthermore, the analysis of discrete-time filters in the discrete-time domain provides a better insight on how their discrete nature affects the front-end noise. The proposed analysis can produce closed-form expressions for the ENC calculation, which can be used for efficient algorithms for the ENC evaluation and filter optimization procedures.

In order to validate the proposed framework in this work, an example is developed, and the result obtained is analyzed and compared with the result provided by the continuous-time approach. Also, an example of optimal filter computation is presented to demonstrate the capabilities of the proposed framework.

3.2 Discrete-Time Analysis

Figure 3.1 shows a simplified model to compute the output-referred noise contribution of a single noise source in a typical front-end detector. It consists of a linear block with a transfer function $H(s)$ that models the effect of the CSA on the noise source under analysis, and a pulse shaper, which in this case is a finite impulse response (FIR) filter with a discrete-time transfer function given by

$$F(z) = \sum_{j=0}^{N-1} a_{N-j}\, z^{-j} \tag{3.1}$$

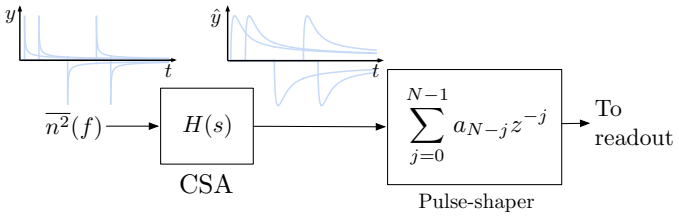

FIGURE 3.1. Model for noise analysis in a typical front-end circuit.

where a_{N-j} are arbitrary coefficients and N is the filter length. The noise source is characterized by its two-sided power spectral density (PSD) $\overline{n^2}(f)$.

For this analysis it is not necessary to consider the details of the physical processes that cause the noise. It will be assumed that the noise source is an arbitrary white or filtered white noise source, which represents any of the fundamental noise sources present at a detector front-end circuit, such as thermal noise, shot noise and flicker noise. This assumption allows to model the noise source in the time domain in terms of a sequence of noise pulses with core function $y(t)$, arriving Poissonianly at times t_a with an average rate ν and random sign (Goulding, 1972; Radeka, 1988). A general procedure to calculate a function $y(t)$ that represents the noise process characterized by $\overline{n^2}(f)$ can be found in (Pullia & Riboldi, 2004).

By using the CSA transfer function and $y(t)$, the effect of an individual noise pulse at the filter input can be determined as

$$\hat{y}(t) = y(t) * \mathcal{L}^{-1}\{H(s)\}(t). \tag{3.2}$$

Both sequences of pulses, at the input and at the output of $H(s)$, are illustrated in Figure 3.1.

Assuming a periodic, synchronous front-end, where the stimulus arrival time within each frame is fixed and known, the CSA can be reset at the beginning of each frame, prior to the corresponding stimulus. Thus, the analysis can be carried out considering a non-stationary noise process that starts at $t = 0$. Then the total integrated noise at the filter input is a function of time (Radeka, 2011). Using (3.2) and Campbell's theorem, the

following expression for the total integrated noise at the filter input can be derived:

$$\sigma^2(t) = \nu \int_0^t \hat{y}^2(t - t_a)\ \mathrm{d}t_a. \tag{3.3}$$

Let us define P_i as the time interval between an arbitrary sample i and its predecessor, given by $P_i = [(i-1)T_s, iT_s]$, where T_s is the filter sampling period. Now consider the noise contribution of the pulses originated within P_i and measured at an arbitrary sample k (i.e., $t = kT_s$), $\sigma_i^2(k)$, as shown in Figure 3.2. Using Campbell's theorem, $\sigma_i^2(k)$ can be computed as

$$\sigma_i^2(k) = \nu \int_{(i-1)T_s}^{iT_s} \hat{y}^2(kT_s - t_a)\ \mathrm{d}t_a\,. \tag{3.4}$$

It can be shown that (3.4), can be expressed as

$$\sigma_i^2(k) = \int_0^{T_s} \hat{y}^2\left(\left(k - i + 1\right) T_s - \eta_1\right)\ \mathrm{d}\eta_1 \tag{3.5}$$

where $\eta_1 = t_a + T_s - iT_s$. This integral can be split into two integrals as follows

$$\begin{aligned}\sigma_i^2(k) = &\int_0^{(k-i+1)T_s} \hat{y}^2\left(\left(k - i + 1\right) T_s - \eta_1\right)\ \mathrm{d}\eta_1 \\ &- \int_{T_s}^{(k-i+1)T_s} \hat{y}^2\left(\left(k - i + 1\right) T_s - \eta_2\right)\ \mathrm{d}\eta_2.\end{aligned} \tag{3.6}$$

Defining $\eta_2 = \eta_3 + T_s$, (3.6) can be written as

$$\begin{aligned}\sigma_i^2(k) \;\; = \;\; &\int_0^{(k-i+1)T_s} \hat{y}^2\left(\left(k - i + 1\right) T_s - \eta_1\right)\ \mathrm{d}\eta_1 \\ &- \int_0^{(k-i)T_s} \hat{y}^2\left(\left(k - i\right) T_s - \eta_3\right)\ \mathrm{d}\eta_3.\end{aligned} \tag{3.7}$$

Since $\hat{y}^2(t)$ is zero for negative arguments, then $\sigma_i^2(k) = 0$ for $k < i$. For $k \geq i$, and according to (3.3), (3.7) can be alternatively expressed as

$$\sigma_i^2(k) = \sigma^2\left(\left(k - i + 1\right) T_s\right) - \sigma^2\left(\left(k - i\right) T_s\right) \tag{3.8}$$

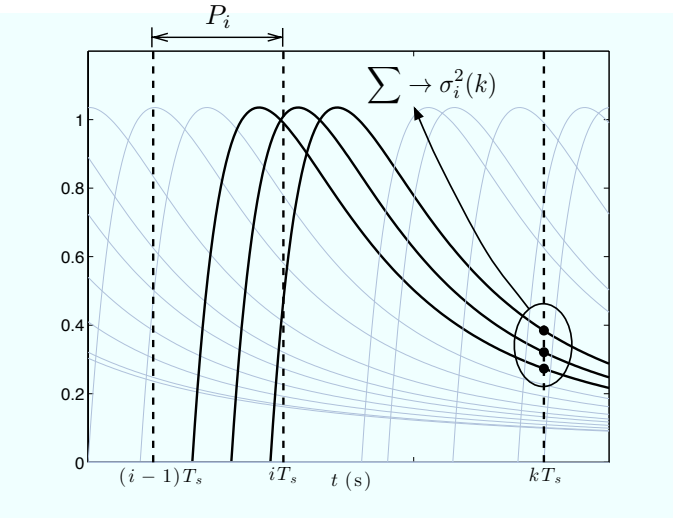

FIGURE 3.2. Noise contribution of the pulses generated within P_i and measured at an arbitrary sample k (i.e., $t = kT_s$), using an arbitrary filtered noise core function $\hat{y}(t)$. The independent contribution of each pulse is pointed out with black dots.

therefore

$$\sigma_i^2(k) = \begin{cases} \sigma^2((k-i+1)T_s) - \sigma^2((k-i)T_s), & k \geq i \\ 0, & k < i. \end{cases} \tag{3.9}$$

Based on (3.9), the total integrated noise at the filter input measured at the k-th sample, $\sigma^2(kT_s)$, can be written as the sum of the individual noise contributions originated at each interval P_i:

$$\sigma^2(kT_s) = \sum_{i=1}^{N} \sigma_i^2(k). \tag{3.10}$$

The evolution of the total integrated noise at the filter input according to (3.10) is illustrated in Figure 3.3.

Since (3.10) is composed by noise contributions originated at different time intervals P_i, the total integrated noise at the filter input holds partial correlation between samples, and the output noise cannot be computed by convolving (3.10) with $F(z)$. However, since all evaluations of $\sigma_i^2(k)$ are originated from the same pulses (for a fixed i), and thus are fully correlated, (3.10) can be split into N independent discrete-time signals

$\sigma_1^2(k), \sigma_2^2(k) \ldots \sigma_N^2(k)$. Each of these signals can be referred to the filter output as

$$\begin{aligned}\hat{\sigma}_i(k) &= \sqrt{\sigma_i^2(k)} * \mathcal{Z}^{-1}\{F(z)\}(k) \\ &= \sum_{j=0}^{k-i} a_{N-j} \sqrt{\sigma_i^2(k-j)}. \end{aligned} \tag{3.11}$$

Signals $\hat{\sigma}_1(k), \hat{\sigma}_2(k) \ldots \hat{\sigma}_N(k)$ are also independent, and can be added up as noise variances to compute the total integrated noise at the filter output as a function of k:

$$\begin{aligned}\hat{\sigma}^2(k) &= \sum_{i=1}^{k} \hat{\sigma}_i^2(k) \\ &= \sum_{i=1}^{k} \left(\sum_{j=0}^{k-i} a_{N-j} \sqrt{\sigma_i^2(k-j)} \right)^2. \end{aligned} \tag{3.12}$$

Evaluating (3.12) at the measurement time $t_m = NT_s$ (i.e., $k = N$) yields

$$\hat{\sigma}^2(N) = \sum_{i=1}^{N} \left(\sum_{j=0}^{N-i} a_{N-j} \sqrt{\sigma_i^2(N-j)} \right)^2. \tag{3.13}$$

Finally, replacing (3.9) in (3.13) and defining $h = N - j - i$, a closed-form expression for the front-end noise can be obtained:

$$\hat{\sigma}^2(N) = \sum_{i=1}^{N} \left(\sum_{h=0}^{N-i} a_{i+h} \sqrt{\sigma^2((h+1)T_s) - \sigma^2(hT_s)} \right)^2. \tag{3.14}$$

The only term of (3.14) that depends on the input-referred noise process is $\sigma^2(t)$, which can be calculated analytically or numerically for typical noise processes by using (3.3). For instance, Figure 3.4 illustrates $\sigma^2(t)$ for thermal, shot and flicker noise. Even though the analysis presented here has been applied for a single noise source, it can be easily extended for circuits with several noise sources by applying the superposition principle in quadrature.

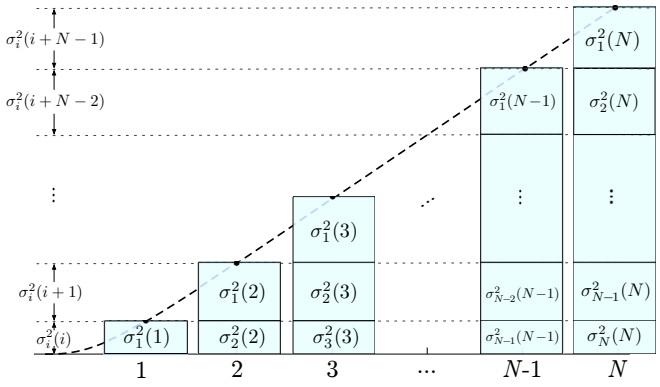

FIGURE 3.3. Evolution of the total integrated noise at the filter input, where the noise of each sample was split according to (3.10).

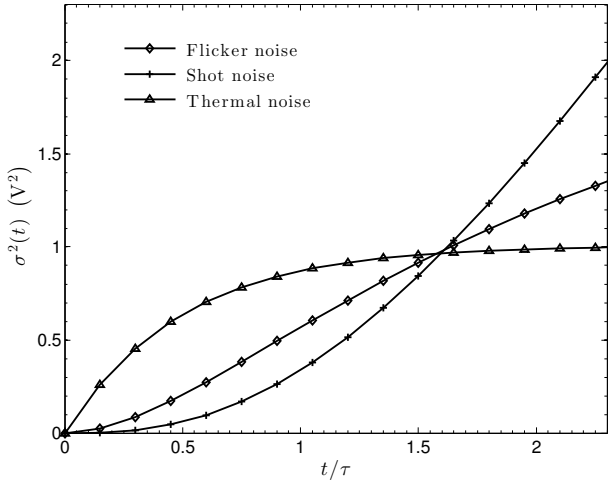

FIGURE 3.4. $\sigma^2(t)$ for thermal, shot and flicker noise with normalized time t/τ and an arbitrary amplitude.

3.3 Example

For validation purposes, the thermal noise contribution at the output of a discrete-time integrator filter will be computed using the proposed discrete-time analysis. The result obtained will be analyzed and then compared with the result produced by the traditional continuous-time approach. Figure 3.5 shows the front-end circuit used for general noise analysis. The detector is modeled as capacitance C_D, whereas the CSA is shown as a

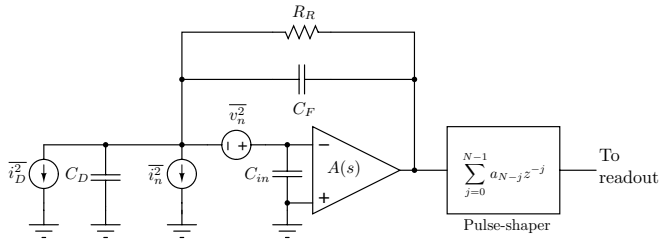

FIGURE 3.5. Front-end circuit used for noise analysis.

voltage amplifier with open loop gain $A(s) = A/(1 + s\tau)$, input capacitance C_{in} and a feedback capacitor C_F. Resistor R_R across the feedback capacitor C_F represents the CSA reset element. The filter coefficients are $a_i = 1$. The detector shot noise represented by $\overline{i_D^2}$ will be omitted for the purpose of this example. Thermal noise has been assumed to be dominated by the CSA input device and is represented by two fully-correlated noise sources (Sansen & Chang, 1990), a voltage white noise source with a two-sided PSD $\overline{v_n^2}$ and a current noise source with a two-sided PSD $\overline{i_n^2}$. Both noise sources are related as follows:

$$\overline{i_n^2} = (sC_{in})^2 \, \overline{v_n^2}. \tag{3.15}$$

Considering that the effect of the reset switch during the relatively short time that it takes the CSA to produce an output voltage is negligible, R_R can be assumed to be infinite (Pullia & Riboldi, 2004). The CSA open loop DC gain (A) is assumed to be very large as well. Under these assumptions and using (3.15), the PSD of the thermal noise referred to the CSA output, $\overline{v_o^2}$, can be approximated to

$$\overline{v_o^2} \approx \left| \frac{C_{tot}}{C_f} \frac{1}{1 + s\hat{\tau}} \right|^2 \overline{v_n^2} \tag{3.16}$$

where $C_{tot} = C_D + C_F + C_{in}$ and $\hat{\tau} = (\tau/A)(\, C_{tot}/C_f)$ is the CSA closed-loop time-constant.

The PSD in (3.16) can be treated as the result of passing a fictitious noise source with PSD $\overline{v_n^2}$ through a block with transfer function $H_{\text{th}}(s)$ given by

$$H_{\text{th}}(s) = \frac{C_{tot}}{C_f} \frac{1}{1 + s\hat{\tau}}. \tag{3.17}$$

Since $\overline{v_n^2}$ characterizes a white noise source, it can be modeled as a sequence of Dirac impulses with core function $y_{\text{th}}(t)$ occurring at an arbitrary rate ν and random sign (Pullia & Riboldi, 2004), where $y_{\text{th}}(t)$ is given by

$$y_{\text{th}}(t) = \sqrt{\frac{\overline{v_n^2}}{\nu}}\delta(t). \tag{3.18}$$

Replacing (3.17) and (3.18) in (3.2), each pulse in the sequence can be referred to the CSA output as an exponentially decaying pulse (Pullia & Riboldi, 2004) as follows

$$\hat{y}_{\text{th}}(t - t_a) = \sqrt{\frac{\overline{v_n^2}}{\nu}}\frac{C_{tot}}{C_F}\frac{e^{-(t-t_a)/\hat{\tau}}}{\hat{\tau}}u(t - t_a) \tag{3.19}$$

where $u(t)$ is the unit step function. Substituting (3.19) in (3.3), the filter input total integrated noise due to the thermal noise, $\sigma_{\text{th}}^2(t)$, can be derived:

$$\sigma_{\text{th}}^2(t) = \overline{v_n^2}\frac{C_{tot}^2}{C_F^2}\frac{1 - e^{-2t/\hat{\tau}}}{2\hat{\tau}}u(t). \tag{3.20}$$

Finally, replacing (3.20) in (3.14) and defining $x = e^{T_s/\hat{\tau}}$, the front-end noise, $\hat{\sigma}_{\text{th}}^2(N)$, can be obtained:

$$\hat{\sigma}_{\text{th}}^2(N) = \frac{\overline{v_n^2}}{2\hat{\tau}}\frac{C_{tot}^2}{C_F^2}\frac{\left(N(x^2-1) - 2x - x^{-2N} + 2x^{-N} + 2x^{1-N} - 1\right)}{(x-1)^2}. \tag{3.21}$$

When the time interval between samples is large enough to consider that consecutive noise samples are uncorrelated (i.e., $\hat{\tau} \ll T_s$), $\hat{\sigma}_{\text{th}}^2(N)$ can be approximated without the use of the proposed analysis as a weighted sum of the uncorrelated samples of the total integrated noise at the CSA output as follows:

$$\hat{\sigma}_{\text{th}}^2(N)\big|_{\hat{\tau} \ll T_s} \approx N \lim_{t\to\infty} \sigma^2(t) = N\frac{\overline{v_n^2}}{2\hat{\tau}}\frac{C_{tot}^2}{C_F^2}. \tag{3.22}$$

As shown in Figure 3.6, (3.21) behaves as predicted by (3.22) for small values of $\hat{\tau}$.

Now, the same example will be analyzed using the traditional continuous-time approach. Using (3.19), the WF $w(t)$, defined as the contribution of each pulse occurring at

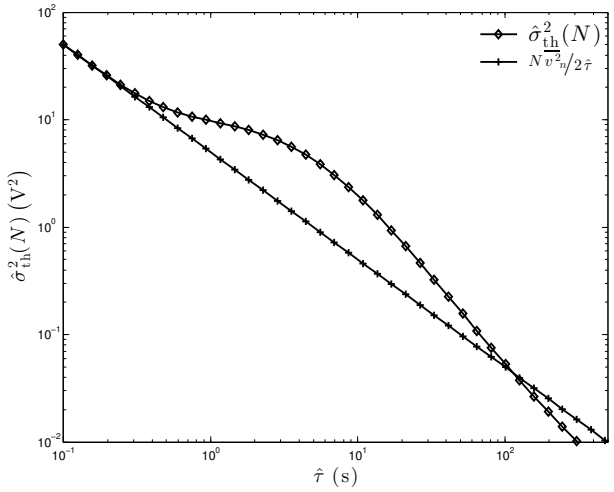

FIGURE 3.6. $\hat{\sigma}^2_{\text{th}}(N)$ and $N\frac{\overline{v_n^2}}{2\hat{\tau}}\frac{C_{tot}^2}{C_F^2}$ as a function of $\hat{\tau}$, using $\overline{v_n^2}=1, C_{tot}^2/C_F^2=1$ and $N=20$.

time t measured at a fixed time $t_m = NT_s$ at the output of the filter, is given by

$$\begin{aligned} w(t) &= \sum_{n=1}^{N} \hat{y}_{\text{th}}(nT_s - t) \\ &= \sqrt{\frac{\overline{v_n^2}}{\nu}}\frac{C_{tot}}{C_F}\sum_{n=1}^{N}\frac{e^{-(nT_s-t)/\hat{\tau}}}{\hat{\tau}}u(nT_s-t). \end{aligned} \tag{3.23}$$

Integrating (3.23) from the reset time ($t=0$) to the signal measurement time ($t=t_m$), the filter total integrated noise at $t=t_m$ can be computed as

$$\begin{aligned} \hat{\sigma}^2_{\text{th}}(N) &= \nu\int_0^{t_m} w^2(t)\,\mathrm{d}t \\ &= \overline{v_n^2}\frac{C_{tot}^2}{C_F^2}\int_0^{NT_s}\left(\sum_{n=1}^{N}\frac{e^{-(nT_s-t)/\hat{\tau}}}{\hat{\tau}}u(nT_s-t)\right)^2\mathrm{d}t. \end{aligned} \tag{3.24}$$

Defining $\alpha = T_s/\hat{\tau}$ and $\beta = t/\hat{\tau}$, (3.24) can be re-written as

$$\hat{\sigma}^2_{\text{th}}(N) = \frac{\overline{v_n^2}}{\hat{\tau}}\frac{C_{tot}^2}{C_F^2}\int_0^{N\alpha} e^{2\beta}\left(\sum_{n=1}^{N} e^{-n\alpha}u\left(n\alpha-\beta\right)\right)^2\mathrm{d}\beta \tag{3.25}$$

which can be split into a sum of integrals as follows

$$\hat{\sigma}^2_{\text{th}}(N) = \frac{\overline{v_n^2}}{\hat{\tau}} \frac{C_{tot}^2}{C_F^2} \sum_{n=1}^{N} \int_{(n-1)\alpha}^{n\alpha} e^{2\beta} \left(\sum_{k=n}^{N} e^{-k\alpha} \right)^2 \mathrm{d}\beta. \tag{3.26}$$

Finally, defining $x = e^{\alpha}$ it can be shown that (3.26) is equal to (3.21).

3.4 ENC Minimization

For filter optimization purposes, a typical front-end circuit with thermal, shot and flicker noise components is considered. The front-end configuration from Figure 3.5 will be used. In this case, the pulse shaper is a discrete-time FIR filter with indeterminate coefficients a_i. Shot noise is assumed to be dominated by the detector noise and is represented by a white noise current source with two-sided PSD $\overline{i_D^2}$ in parallel with the detector capacitance C_D and given by

$$\overline{i_D^2} = qI_L \tag{3.27}$$

where q is the electron charge and I_L the detector leakage current. Thermal noise and flicker noise are assumed to be dominated by the noise of the CSA input device and are represented by two fully-correlated noise sources, a voltage noise source with two-sided PSD $\overline{v_n^2}$ given by

$$\overline{v_n^2} = a_T + \frac{a_F}{|f|} \tag{3.28}$$

where a_T and a_F are the thermal and flicker coefficients, and a current noise source with two-side PSD $\overline{i_n^2}$ given by (3.15). Traditionally, the coefficients a_T and a_F are obtained from the CSA input device models. However, for design purposes the most accurate values shall be used, and these coefficients should be extracted from experiments (Bertuccio & Pullia, 1993) or precise simulations.

Considering the contribution of each noise process separately, the ENC^2 for the output measured at $t = NT_s$ can be written as

$$ENC^2 = \frac{\hat{\sigma}^2_{\text{shot}}(N) + \hat{\sigma}^2_{\text{th}}(N) + \hat{\sigma}^2_{1/f}(N)}{q^2 \left|\max[w(t)]\right|^2 / C_F^2} \tag{3.29}$$

where $\hat{\sigma}^2_{\text{shot}}(N)$ is the shot noise contribution, $\hat{\sigma}^2_{\text{th}}(N)$ is the thermal noise contribution, $\hat{\sigma}^2_{1/f}(N)$ is the flicker noise contribution and $w(t)$ is the weighting function at the front-end output given by (3.23).

In order to find the coefficients a_i that minimize (3.29), and hence the optimal FIR filter, the signal measurement time $t_m = NT_s$ was assumed to be a constant determined by the processing time budget constraints, and the filter sampling period T_s was assumed to be a constant determined by the filter maximum clock rate. Although $\hat{\tau}$ is a design variable that depends on the CSA and not on the filter, it has been included in the optimization analysis.

Given that a common WF reaches its maximum value at $t = t_m/2$, and that the WF height is commonly a design constraint, the denominator of (3.29) was forced to be constant by fixing the WF height, h_w, through the following constraints

$$\sum_{i=1}^{N/2} a_i \left(1 - e^{-T_s(N/2-i+1)/\hat{\tau}}\right) = h_w \tag{3.30}$$

$$\sum_{i=1}^{N} a_i \left(1 - e^{-T_s(N-i+1)/\hat{\tau}}\right) = 0. \tag{3.31}$$

Although these constraints appear from foreknowledge about the shape of the optimum WF, the actual computation of $w(t)$ was never required for the optimization problem formulation. For illustration purposes, the length of the filter N was assumed to be an even number. Considering these constraints, minimizing the ENC^2 is equivalent to minimizing

its numerator, and according to (3.14), the resulting objective function f_o is given by

$$f_o = \sum_{i=1}^{N} \left\{ \left(\sum_{h=0}^{N-i} a_{i+h} \sqrt{\sigma^2_{\text{shot}}((h+1)T_s) - \sigma^2_{\text{shot}}(hT_s)} \right)^2 + \left(\sum_{h=0}^{N-i} a_{i+h} \sqrt{\sigma^2_{\text{th}}((h+1)T_s) - \sigma^2_{\text{th}}(hT_s)} \right)^2 + \left(\sum_{h=0}^{N-i} a_{i+h} \sqrt{\sigma^2_{1/f}((h+1)T_s) - \sigma^2_{1/f}(hT_s)} \right)^2 \right\}. \tag{3.32}$$

To obtain a numerical solution for the optimization problem, given by the objective function (3.32) and constraints (3.30) and (3.31), the parameters of an HPGe segmented detector with an input FET transistor were considered. Assuming that the input device is in strong inversion, the coefficient a_T can be calculated as

$$a_T = \frac{2KT\gamma}{g_m} \tag{3.33}$$

where K is the Boltzmann constant, T is the absolute temperature, g_m is the transconductance of the input device and γ is a constant factor, typically $\approx 2/3$ (Van Der Ziel, 1970). The following parameters, typical of an HPGe segmented detector (Pullia & Riboldi, 2004), were used: $T = 120\,\text{K}$, $g_m = 15\,\text{mS}$, $R_F = 1\,\text{G}\Omega$, $I_L = 100\,\text{pA}$, $C_T = 40\,\text{pF}$, $C_F = 1\,\text{pF}$ and $a_F = 10^{-15}\,\text{V}^2$. Additionally, the following parameters were arbitrarily selected: $t_m = 10\,\mu\text{s}$, $T_s = 0.5\,\mu\text{s}$ and $h_w = 1$.

The optimization problem was formulated in MATLAB and then solved through convex optimization with CPLEX (IBM, n.d.). Figure 3.7 shows the optimum value of the ENC^2 as a function of $\hat{\tau}$, where the existence of a global optimum at $\hat{\tau} = 0.184\,\mu\text{s}$ can be seen. Figure 3.8 shows the optimum WF for different values of $\hat{\tau}$. Using the optimum WF and the noise parameters shown above the ENC can be computed as described in (Gatti & Manfredi, 1986) and (Pullia, 1998).

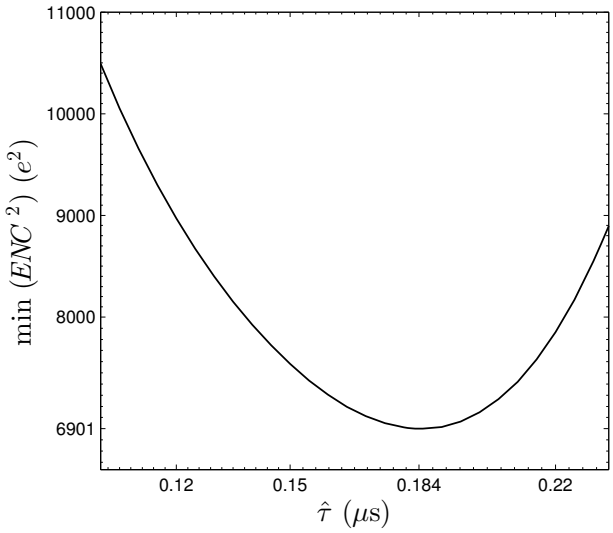

FIGURE 3.7. Minimum ENC^2 as a function of $\hat{\tau}$ for a fixed N.

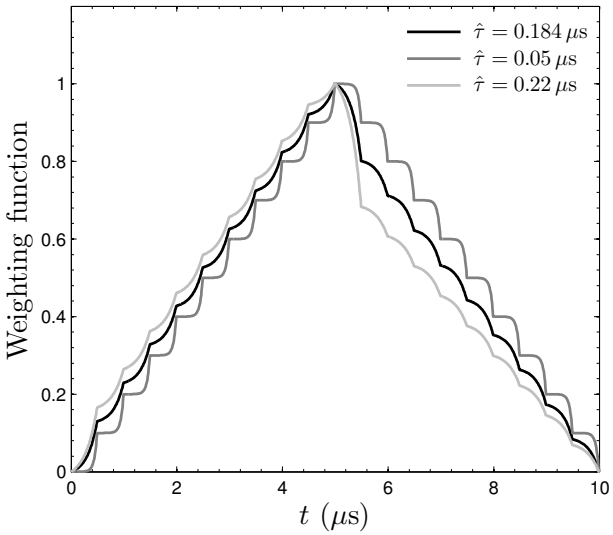

FIGURE 3.8. Optimum WF for different values of $\hat{\tau}$ for $N = 20$.

The initial assumption that the filter sampling period T_s is determined by the filter maximum clock rate is only valid if the optimum ENC^2 is lower bounded by T_s, or equivalently, by N. To support this assumption, Figure 3.9 shows the optimum value of the ENC^2 as a function of N. Although Figure 3.9 suggests to use the filter at the maximum

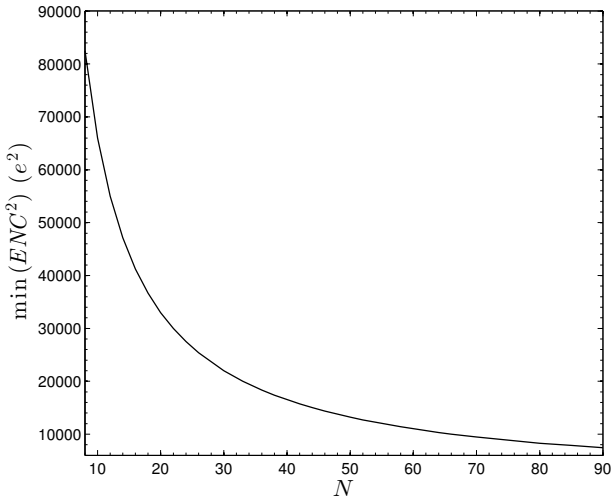

FIGURE 3.9. Optimum ENC^2 as a function of N for $\hat{\tau} = 0.03\,\mu$s.

clock rate, for a large number of samples the contribution of an additional sample is marginal, thus to determine N other considerations should be taken into account, such as the filter power consumption and the filter design complexity. Additional requirements, such as flat-top or zero-area, can be easily added as constraints in the optimization problem.

3.5 Conclusion

This work presents a mathematical framework for the analysis of discrete-time filters in the discrete-time domain. The analysis is based on decomposing the total integrated noise at the filter input into a set of discrete-time noise signals, in order to refer them to the filter output and calculate the ENC. The proposed analysis only depends on the calculation of the total integrated noise at the filter input, which can be analyzed prior to taking into account the filter itself in order to understand and predict the noise behavior.

In order to validate the proposed framework, the computation of the thermal noise contribution at the output of a discrete-time integrator is presented, and the result is compared to the result produced by the traditional continuous-time approach. Although both methods produce mathematically equivalent results, the former is simpler and more insightful.

This work also presents an example of optimal filter computation, in order to demonstrate the proposed framework capabilities and its application to optimization problems with several noise sources.

4. A SC FILTER FOR ARBITRARY WEIGHTING FUNCTION SYNTHESIS

4.1 Introduction

4.1.1 Filter Specifications

4.2 System-Level Design

4.3 Circuit Design

4.3.1 Operational Transconductance Amplifier

4.3.2 Capacitor Array

4.3.3 Rail-to-Rail buffer

4.3.4 Bias networks

5. RESULTS

5.1 Filter simulation results

5.1.1 OTA simulations results

5.1.2 Rail-to-rail buffer simulations results

5.1.3 Arbitrary weighting function synthesis

5.2 The Bean V2 Prototype

5.2.1 Floorplan

6. CONCLUSION

6.1 Summary

6.2 Future work

7. THE BEAN V2 PINOUT

References

Abusleme, A., Dragone, A., Haller, G., & Wooley, B. (2012). Beamcal Instrumentation IC: Design, Implementation, and Test Results. *IEEE Trans. Nucl. Sci.*, *59*(3), 589-596.

Bertuccio, G., & Pullia, A. (1993). A method for the determination of the noise parameters in preamplifying systems for semiconductor radiation detectors. *Rev. Sci. Instrum*, *64*(11), 3294-3298.

De Geronimo, G., & O'Connor, P. (2005). MOSFET optimization in deep submicron technology for charge amplifiers. *IEEE Trans. Nucl. Sci.*, *52*(6), 3223-3232. doi: 10 .1109/TNS.2005.862938

Fiorini, C., & Buttler, W. (2002). Multicorrelated double sampling readout of asynchronous events from multi-element semiconductor detectors. *IEEE Trans. Nucl. Sci.*, *49*(3), 1566-1573.

Gatti, E., Geraci, A., & Ripamonti, G. (1996). Automatic synthesis of optimum filters with arbitrary constraints and noises: a new method. *Nucl. Instrum. and Meth.*, *A381*(1), 117-127.

Gatti, E., & Manfredi, P. (1986). Processing the signals from solid-state detectors in elementary-particle physics. *Riv. Nuovo Cim.*, *9*, 1-146. doi: 10.1007/BF02822156

Geraci, A., & Gatti, E. (1995). Optimum filters for charge measurements in the presence of 1/f current noise. *Nucl. Instrum. and Meth.*, *A361*(2), 277-289.

Geraci, A., Zambusi, M., & Ripamonti, G. (1996). A comparative study of the energy resolution achievable with digital signal processors in X-ray spectroscopy. *IEEE Trans. Nucl. Sci.*, *43*(2), 731-736.

Geronimo, G. D., O'Connor, P., Radeka, V., & Yu, B. (2001). Front-end electronics for imaging detectors. *Nucl. Instrum. and Meth.*, *A471*(12), 192-199. doi: 10.1016/S0168-9002(01)00963-9

Goulding, F. (1972). Pulse-shaping in low-noise nuclear amplifiers: A physical approach to noise analysis. *Nucl. Instrum. and Meth.*, *100*(3), 493-504. doi: 10.1016/0029-554X(72)90828-2

IBM. (n.d.). *ILOG CPLEX Optimizer*. Retrieved from `http://www.ilog.com/products/cplex/`

Jordanov, V. T. (2003). Real time digital pulse shaper with variable weighting function. *Nucl. Instrum. and Meth.*, *A505*(1), 347-351.

Livingston, M., & Blewett, J. (1962). *Particle accelerators*. McGraw-Hill. Retrieved from `http://books.google.cl/books?id=Hi9RAAAAMAAJ`

Porro, M., Herrmann, S., & Hornel, N. (2007). Multi correlated double sampling with exponential reset. In *IEEE nucl. sci. symp. conf. rec* (Vol. 26, p. 291-298).

Pullia, A. (1997). How to derive the optimum filter in presence of arbitrary noises, time-domain constraints, and shaped input signals: A new method. *Nucl. Instrum. and Meth.*, *A397*, 414-425. doi: 10.1016/S0168-9002(97)00778-X

Pullia, A. (1998). Impact of non-white noises in pulse amplitude measurements: a time-domain approach. *Nucl. Instrum. and Meth.*, *A405*(1), 121-125.

Pullia, A., & Gatti, E. (2002). Optimal filters with constant-slope crossover and finite width for pulse-timing measurements. *IEEE Trans. Nucl. Sci.*, *49*(3), 1170-1176.

Pullia, A., & Riboldi, S. (2004). Time-domain Simulation of electronic noises. *IEEE Trans. Nucl. Sci.*, *51*(4), 1817-1823. doi: 10.1109/TNS.2004.832564

Radeka, V. (1968). Optimum Signal-Processing for Pulse-Amplitude Spectrometry in the Presence of High-Rate Effects and Noise. *IEEE Trans. Nucl. Sci.*, *15*(3), 455-470.

Radeka, V. (1988). Low-Noise Techniques in Detectors. *Ann. Rev. Nucl. Part. Sci*, *38*(1), 217-277. doi: 10.1146/annurev.ns.38.120188.001245

Radeka, V. (2011). Signal Processing for Particle Detectors. In C. Fabjan & H. Schopper (Eds.), *Detectors for Particles and Radiation. Part 1: Principles and Methods* (Vol. 21B1, p. 288-319). Springer Berlin Heidelberg. doi: 10.1007/978-3-642-03606-4_10

Sampietro, M., Bertuccio, G., Geraci, A., & Fazzi, A. (1995). A digital system for "optimum" resolution in x-ray spectroscopy. *Rev. Sci. Instrum*, *66*(2), 975-981.

Sansen, W., & Chang, Z. (1990). Limits of low noise performance of detector readout front ends in CMOS technology. *IEEE Trans. Circuits Syst.*, *37*(11), 1375-1382. doi: 10.1109/31.62412

Tuttle, K. (2013). Why particle physics matters. *Symmetry Magazine*.

Van Der Ziel, A. (1970). Noise in solid-state devices and lasers. *Proc. of IEEE*, *58*(8), 1178-1206.

APPENDIX

A. THE BEAN V2 PINOUT